S_H2 Reaction vs Hydrogen Abstraction/Expulsion in Methyl Radical−Methylsilane Reactions: Effects of Prereactive Complex Formation

Daniel Norberg,[†] Masaru Shiotani,[‡] and Sten Lunell*[,†]

Department of Quantum Chemistry, Uppsala University, Box 518, SE-751 20 Uppsala, Sweden, and Department of Applied Chemistry, Graduate School of Engineering, Hiroshima University, 4-1, Kagamiyama 1, Higashi-Hiroshima 739-8527, Japan

Received: August 16, 2007; In Final Form: November 27, 2007

A quantum chemical study has been undertaken to elucidate the cause of the recently observed S_H2 reaction between the deuterated methyl radical ($^{\bullet}CD_3$) and methylsilane (SiD_3CH_3) following the photolysis of CD_3I. [Komaguchi, K.; Norberg, D.; Nakazawa, N.; Shiotani, M.; Persson, P.; Lunell, S. *Chem. Phys. Lett.* **2005**, *410*, 1−5.] It is found that the backside S_H2 mechanism may proceed favorably for C−Si−C angles deviating with up to 40° from linearity. The competitive hydrogen abstraction reaction is predicted to be active in the range of 90° ≤ C−Si−C ≤ 135°. For steeper attack angles, the frontside S_H2 mechanism is activated. However, high barriers along the corresponding reaction paths probably make the frontside mechanism less important for the present S_H2 reaction. A number of bound SiH_3CH_3/CH_3I complexes have been located with the MP2 method. At the CCSD(T) level, a complex corresponding to the collinear arrangement where the methyl moiety of methyl iodide points toward the silicon, which is the most favorable conformation for the subsequent S_H2 reaction with the backside mechanism, is found to be the most stable linear conformer. A complex with similar energy is found where the methyl moiety of methyl iodide points approximately toward an Si−H bond. However, because C−Si−C = 69.4° in this complex, subsequent photolysis of methyl iodide would probably not lead to hydrogen abstraction with full efficiency. These findings could provide an explanation for the observed S_H2 reaction.

Introduction

Bimolecular homolytic substitution (S_H2) reactions[1−4] (eq A) play important roles in radical chemistry and have been regarded as an important tool in synthesis[5] because of the elemental steps available for free radicals ($R_1^{\bullet}$) to generate a new radical ($R_2^{\bullet}$). The most common reactions of S_H2 type are the abstraction

$$R_1^{\bullet} + A{-}R_2 \rightarrow R_1{-}A + R_2^{\bullet} \qquad (A)$$

reactions of hydrogen or halogen at monovalent centers. However, it is known that more complex S_H2 reactions generally proceed at multivalent centers, which include Si, Ge, and Sn atoms, having low-lying unfilled orbitals.[1−5] The S_H2 reactions have been experimentally studied mainly in the gas phase by means of mass spectroscopy,[6] whereas the studies in solution, especially in low temperature solid solution, are quite limited.[7,8]

Recently, we observed the S_H2 reaction between the deuterated methyl radical ($^{\bullet}CD_3$) and SiD_3CH_3 (eq B) by means of electron spin resonance (ESR) spectroscopy.[7] The ESR experiments were carried out at low temperatures for a solid solution containing *ca.* 1 mol % of methyl iodide in solid methylsilane and the methyl radicals were generated by photolysis of methyl iodide. The ESR spectra revealed that the S_H2 reaction (B) proceeded at a low temperature of 77 K with high selectivity over the competitive deuterium abstraction, at the initial stage of the reaction. On the other hand, only the product of hydrogen abstraction, the methylsilyl radical ($^{\bullet}SiH_2CH_3$), could be observed for the unlabeled compounds (eq C). It was suggested that slow deuterium abstraction, owing to the large kinetic isotope effect observed[9] for the hydrogen abstraction by the methyl radical from methylsilane (k_{Si-H}/k_{Si-D} = 5200, experimental value at 77 K), made it possible to observe the S_H2 reaction (B); the observed large isotope effect revealed that the quantum mechanical tunneling effect significantly contributes to the H atom abstraction by CH_3 radicals from the $-SiH_3$ group, especially at low temperatures.

$$CH_3SiD_3 + {}^{\bullet}CD_3 \rightarrow {}^{\bullet}CH_3 + SiD_3CD_3 \qquad (B)$$

$$CH_3SiH_3 + {}^{\bullet}CH_3\ (\text{or } {}^{\bullet}CD_3) \rightarrow CH_3SiH_2^{\bullet} + CH_4\ (\text{or } CD_3H) \qquad (C)$$

The S_H2 reaction between the unlabeled methyl radical and methylsilane has been extensively investigated theoretically by Schiesser and co-workers.[10,11] They considered two possible conformations for the transition structure (TS) of this reaction, one that is collinear, and one that is bent with respect to the C−Si−C angle. These conformations define the backside and frontside mechanisms for the S_H2 reaction, respectively.

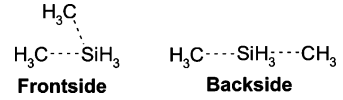

Ab initio calculations have suggested that the backside and frontside mechanisms are competitive for the S_H2 reaction between the methyl radical and XH_3YH_3, where X and Y are Si, Ge, or Sn.[12] However, whereas the backside TS for the

* Corresponding author. E-mail: Sten.Lunell@kvac.uu.se.
† Uppsala University.
‡ Hiroshima University.

10.1021/jp076591y CCC: $40.75
Published on Web 01/17/2008

present S_H2 reaction was successfully located at all levels of theory employed,[10] the frontside TS could only be obtained at the uncorrelated Hartree−Fock (HF) level.[11] In particular, optimization of the frontside TS with MP2, using a variety of basis sets, collapsed to a TS for expulsion of one of the hydrogen atoms at silicon.[11]

In our previous computational investigation of the reactions between the methyl radical and methylsilane, we located channels for the backside S_H2 reaction (B) and the hydrogen abstraction (C).[7] For the unlabeled compounds, the zero-point vibrational energy (ZPVE) corrected activation energies of the former and latter reactions were predicted to be 22.7 and 8.8 kcal mol^{-1}, respectively, at the CCSD(T)/AUG-cc-pVDZ//B3LYP/6-31+G(d,p) level of theory. Moreover, the hydrogen abstraction was found to be exothermic by 12.4 kcal mol^{-1}. Similar values were obtained for the two channels for all of the deuterium substituted compounds. In particular, the barriers for the S_H2 reaction (B) and for the corresponding deuterium abstraction were predicted to be 22.0 and 8.8 kcal mol^{-1}, respectively. Hence, our calculations indicated that hydrogen abstraction should be the favored reaction regardless of the isotopic identity of the hydrogen atoms. Nevertheless, an estimation of the translational kinetic energy of the methyl radical following photolysis of methyl iodide, ∼22 kcal mol^{-1}, showed that the reaction in eq B might proceed given a favorable initial orientation of methylsilane and methyl iodide.[7]

In this work, we continue to explore the cause of the observed S_H2 reaction between the methyl radical and methylsilane by means of quantum chemical calculations. In particular, we investigate further the potential energy surface (PES) governing the methyl radical attack on silicon in methylsilane from different C−Si−C angles. Moreover, an extensive search for SiH_3CH_3/CH_3I complexes is undertaken to investigate different molecular arrangements of the reactants prior to photolysis.

Computational Details

All quantum chemical calculations have been performed with the Gaussian03 suite of programs.[13] The molecular pictures were obtained with Molekel.[14] The geometries of the stationary points involved in the reactions between the methyl radical and methylsilane were optimized with B3LYP in conjunction with the 6-311+G(d,p) basis set. At this level, ZPVEs were obtained. Electronic energies were subsequently computed with CCSD(T)/6-311+G(d,p) on these optimized stationary points. The vibrational frequency spectra of the stationary points were inspected and it was made sure that minima had zero imaginary frequencies and that transition structures had one. Moreover, the imaginary normal modes were analyzed to verify that they corresponded to the correct distortions of the molecular structure, leading from reactants to products.

In general, DFT is not well suited for the prediction of geometries and energies of weakly interacting systems.[15−18] This can in part be explained by the fact that dispersion becomes important for such nonbonded interactions and the current DFT methods are not explicitly designed to treat dispersion.[19] Instead, correlated *ab initio* methods are preferable in these cases. Nevertheless, due to the advantage of DFT compared to, *e.g.*, MP2, with regard to computational time requirements, DFT would be preferable for the preliminary investigation of the PES. Indeed, in a recent evaluation of the performance of a large number of DFT methods for predicting binding energies of nonbonded complexes, some functionals were found to be comparable to MP2 for this purpose.[19] In particular, the B97-1 method was found to be the best DFT functional for the prediction of binding energies of complexes in which the nonbonded interactions were dominated by dispersion or by dipolar interactions.[19] Therefore, we chose B97-1 for the preliminary investigation of different complexes formed between methylsilane and methyl iodide in the present work. For consistency with the evaluation,[19] the B97-1 functional was used in conjunction with the 6-311+G(2df,2p) basis set for the H, C and Si atoms whereas the LanL2DZ basis set was used to describe the iodine atoms. The B97-1 optimized complexes were subsequently re-optimized with MP2, using the same basis set, which hence is our production level for the geometries. Electronic energies were computed for the MP2 optimized complexes with CCSD(T) in conjunction with both 6-311+G(2df,2p) and 6-311++G(3df,3pd) for the H, C, and Si atoms. The iodine atoms in the CCSD(T) calculations with the larger basis set were described by the LanL2DZ basis set augmented with the d-type polarization and p-type diffuse functions of Check et al.[20] The latter basis set is here referred to as "LanL2DZdp". We have not compensated for the effect of basis set superposition because we are here interested in the energy differences between different complexes of very similar type. Hence, we do not explicitly calculate the binding energies of the complexes, whose magnitudes would be sensitive to basis set superposition effects.

The restricted formalism was employed for closed shell singlets, and the unrestricted formalism was used for radicals of doublet state. The DFT geometries and energies of the SiH_3CH_3/CH_3I complexes were computed with an ultrafine integration grid.[21] Default convergence criterions were used throughout.

Results and Discussion

In this work, we investigated the possible reactions between $^{\bullet}CH_3$ and SiH_3CH_3 when the methyl radical approaches the silicon atom from different C−Si−C angles. We located channels for (1) the backside S_H2 mechanism which exchanges the two methyl radicals, (2) the hydrogen abstraction from silicon, and (3) hydrogen expulsion from silicon *via* the backside S_H2 mechanism leading to formation of dimethylsilane. No TS for the frontside S_H2 mechanism of reaction 1 could be located in the present work. The B3LYP/6-311+G(d,p) optimized TSs

$$CH_3SiH_3 + {}^{\bullet}CH_3 \rightarrow [\mathbf{TS1}]^{\ddagger} \rightarrow {}^{\bullet}CH_3 + SiH_3CH_3 \quad (1)$$

$$CH_3SiH_3 + {}^{\bullet}CH_3 \rightarrow [\mathbf{TS2}]^{\ddagger} \rightarrow CH_3SiH_2^{\bullet} + CH_4 \quad (2)$$

$$CH_3SiH_3 + {}^{\bullet}CH_3 \rightarrow [\mathbf{TS3}]^{\ddagger} \rightarrow CH_3SiH_2CH_3 + H^{\bullet} \quad (3)$$

for reactions 1−3 are displayed in Figure 1, with selected geometrical parameters. The TS for the S_H2 reaction (1), **TS1**, has essentially D_{3h} symmetry and attains a linear conformation with respect to the C−Si−C angle (180.0°). The geometrical parameters in **TS1** are very close to our previously reported values for this TS at the B3LYP/6-31+G(d,p) level of theory.[7] As can be seen in Figure 1, reactions 2 and 3 proceed through TSs, which have much steeper C−Si−C angles; 109.8 and 99.2° for **TS2** and **TS3**, respectively. In **TS2**, the hydrogen H_a is abstracted in an essentially linear conformation with respect to the C_1-H_a-Si angle (179.0°), but it is found that the C_1-Si-H_a angle in **TS3** (166.3°) for expulsion of H_a is significantly bent. It is interesting to note that the main difference between the channels (2) and (3) is the orientation of the methylsilane fragment relative to the attacking methyl radical with C_1. This is reflected by the $C_1-Si-C_2-H_d$ dihedral angle, which is −179.9° and −119.5° in **TS2** and **TS3**, respectively. Hence,

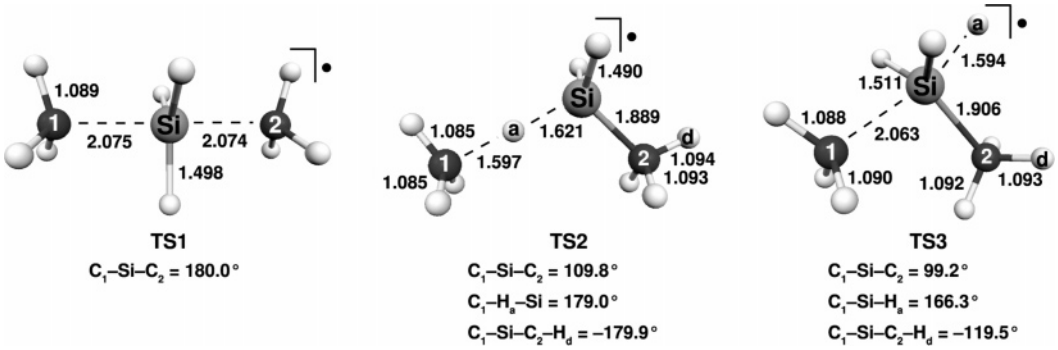

Figure 1. B3LYP/6-311+G(d,p) optimized TSs for reactions 1−3. Bond lengths are given in Ångströms.

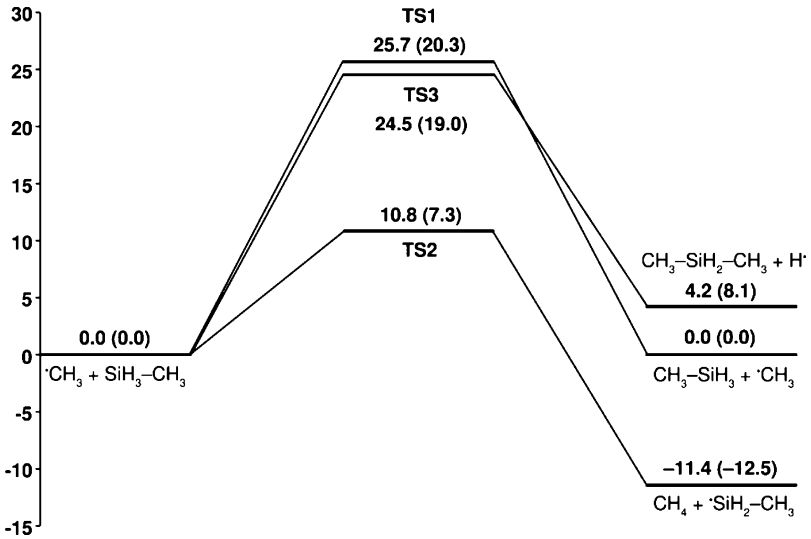

Figure 2. ZPVE corrected CCSD(T)/6-311+G(d,p)//B3LYP/6-311+G(d,p) energy profiles, in kcal mol^{-1}, for reactions 1−3. The ZPVE corrected B3LYP/6-311+G(d,p) relative energies are given within parentheses.

the methylsilane fragment in the TS for hydrogen expulsion from silicon is rotated ca. 60° about the Si−C_2 axis relative to the same fragment in the TS for hydrogen abstraction. Again, the geometrical parameters for **TS2** are found to be close to those predicted previously for this TS with B3LYP/6-31+G-(d,p).[7]

No stable intermediate complexes were found in any of the reaction paths (1)−(3); hence, they are all concerted reactions. For reactions 1 and 2, this is in agreement with our previous results at the B3LYP/6-31+G(d,p) level of theory.[7] However, as we have noted,[7] a concerted mechanism for reaction 1 stands in contrast to the stepwise channel located with MP2/6-311G** by Schiesser et al.[10] who found that the D_{3h} symmetric arrangement corresponded to a shallow minimum and that the TS was slightly distorted away from D_{3h} symmetry in the sense that the C−Si bond distances were unequal.

Potential Energy Profiles for Reactions 1−3. ZPVE corrected energy profiles at the CCSD(T)/6-311+G(d,p)//B3LYP/6-311+G(d,p) level of theory for reactions 1−3 are displayed in Figure 2. For comparison, the ZPVE corrected B3LYP/6-311+G(d,p) relative energies are given within parentheses in this figure. In agreement with our previous investigation,[7] the present calculations predict that the hydrogen abstraction reaction (2) requires much less activation energy, 10.8 kcal mol^{-1}, compared to the S_H2 reaction (1), 25.7 kcal mol^{-1} (the corresponding values for the slightly smaller basis sets used in ref 7 were 8.8 and 22.7 kcal mol^{-1}, respectively). Moreover, whereas the reaction energy of the identity reaction (1) is nil, the hydrogen abstraction is found to be highly exothermic, −11.4 kcal mol^{-1}. It is worthwhile to note that the hydrogen expulsion reaction (3), although not visible in the ESR spectrum,[7] is predicted to proceed through a barrier of 24.5 kcal mol^{-1}, which is lower by 1.2 kcal mol^{-1} than that for the S_H2 reaction (1). However, the former reaction is endothermic by 4.2 kcal mol^{-1}, which makes it less likely to occur. In general, the B3LYP method reproduces the CCSD(T) energy profiles qualitatively, as can be seen in Figure 2. However, the B3LYP barrier heights are consistently underestimated relative to CCSD-(T). Moreover, the hydrogen expulsion reaction (3) is substantially more endothermic (+3.9 kcal mol^{-1}) at the B3LYP level as compared to CCSD(T).

Methyl Radical Attack at Silicon in SiH_3CH_3 from Different C−Si−C Angles. The rather large difference between the C−Si−C angles in the TS for the S_H2 reaction, **TS1** (180.0°), and the TSs for the hydrogen abstraction, **TS2** (109.8°), and the hydrogen expulsion reaction, **TS3** (99.2°), might indicate that the S_H2 reaction (1) could proceed in a wide range of C−Si−C angles before the other channels become activated. To investigate this possibility closer, we performed two sets of 26 constrained optimization scans at the B3LYP/6-31+G(d,p) level where the methyl radical attacks the silicon atom in methylsilane at different C−Si−C angles. Each scan was started from an initial Si−C_1 distance of 5.0 Å (see Figure 3a for the labels), which was then decreased, incrementally by 0.1 Å, to a final value of 1.8 Å. A range of 24 C−Si−C angles from 60° to 175°, with an interval of 5°, was investigated. The two final C−Si−C angles were set to 179° and 179.9°. In one of the sets of scans, the C_1−Si−C_2−H_a dihedral angle was held frozen at 0°. This set of scans is referred to as **D0**. In the second set, referred to as **D180**, the same dihedral angle was held frozen at

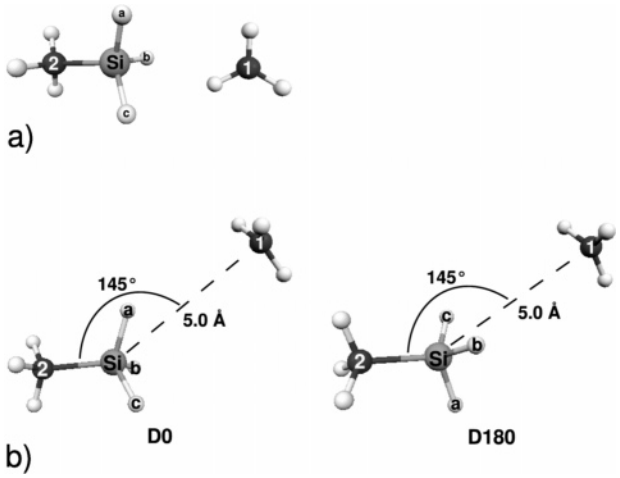

Figure 3. (a) Structures of methylsilane and methyl radical with labels used in the discussion. (b) Initial conformations of the **D0** and **D180** sets of scans with C−Si−C = 145°.

180°. Hence, in both sets of scans, the C_1, C_2, Si, and H_a atoms lie in the same plane. However, in the **D0** set, the methyl radical will approach the Si atom such that abstraction of H_a will have the highest probability to succeed at C−Si−C angles close to 110°. In contrast, in the **D180** set, the methyl radical approaches the Si atom in between two Si hydrogen atoms (H_b and H_c), making hydrogen abstraction least probable for C−Si−C angles close to 110°. The different molecular arrangements for **D0** and **D180** are exemplified in Figure 3b for C−Si−C = 145°.

Potential Energy Surface Formed by the D0 Set of Scans. A 2-dimensional energy profile was constructed from the **D0** set of scans (Figure 4). This energy profile shows how the energy changes *versus* the Si−C_1 distance and the C−Si−C angle. In some of the individual scans, secondary reactions were observed after the methyl radical had reacted with methylsilane. However, because these secondary reactions were found to be associated with high barriers, only points belonging to the primary reactions are included in the energy profile.

As is clear from Figure 4, there are distinct regions on the PES that lead to different products. The various reactions, and the respective C−Si−C angles where they proceed, are given in Table 1. This table also gives the approximate "transition state" energy for each C−Si−C angle, as defined by the highest point on each individual scan energy profile, as well as the Si−C_1 distance where the reaction occurs. For clarity, a picture of methylsilane is introduced in Figure 4, indicating the various reactions and the C−Si−C angles where they proceed.

It is noted that the backside S_H2 reaction (1) proceeds in the range 179.9° ≥ C−Si−C ≥ 145°. Moreover the S_H2 reaction has the highest probability to occur at C−Si−C = 179.9°, where the barrier is 17.1 kcal mol^{-1}, whereas the highest activation energy, 22.6 kcal mol^{-1}, is found at C−Si−C = 145°. This is in good agreement with the linear TS (**TS1**), which was optimized for this reaction.

Proceeding to steeper C−Si−C angles, it is found that at 140°, the reaction between the methyl radical and methylsilane leads to expulsion of one Si hydrogen atom, and to formation of dimethylsilane.

At an attack angle of 135°, the hydrogen abstraction reaction (2) comes into play. This reaction prevails in the range 135° ≥ C−Si−C ≥ 90° and is associated with barriers from 6.0 to 9.8 kcal mol^{-1}. The lowest activation energy for hydrogen abstraction is attained at C−Si−C = 110° (Table 1), which is in agreement with the TS (**TS2**) that was optimized for this reaction.

Interestingly, for the steepest range of angles of attack investigated: 85° ≥ C−Si−C ≥ 60°, the S_H2 reaction (1) again becomes activated, but now *via* the frontside mechanism. However, as can be seen in Table 1 and Figure 4, the corresponding barrier increases steadily from 22.7 to 42.3 kcal mol^{-1} within this range, clearly making the frontside mechanism less energetically favorable than the backside mechanism. Moreover, as mentioned, all attempts of optimizing the TS for the frontside S_H2 reaction with B3LYP failed.

Potential Energy Surface Formed by the D180 Set of Scans. A 2-dimensional energy profile was constructed from the **D180** set of scans (Figure 5) in the same manner as described for the **D0** energy profile. The various reaction types, their barriers, their respective range of angles of attack, and the Si−C_1 distances of where the reactions occur, are given in Table 1. For clarity, a picture of methylsilane is introduced in Figure 5, indicating the various reactions and the C−Si−C angles where they proceed.

Inspection of Table 1 reveals that the backside S_H2 reaction again proceeds at the most obtuse range of C−Si−C angles: 179.9−140°. By analyzing the corresponding barriers, which vary between 18.1 and 21.6 kcal mol^{-1} for this range, we conclude that they are slightly higher for the most linear angles, but slightly lower for the steepest angles, as compared to the backside S_H2 activation energies in the **D0** set of scans.

Further inspection of Table 1 shows that none of the scans in the **D180** set leads to hydrogen abstraction, a fact that can also be confirmed in Figure 5. This can be explained by the fact that the methyl radical approaches the Si atom in between the hydrogens H_b and H_c (Figure 3b). Instead, two other reactions are found to proceed in the range 135° ≥ C−Si−C ≥ 90°. In the range 135−115°, a reaction is observed with barriers of 20.9−19.5 kcal mol^{-1}, which seems to lead to the formation of a hypervalent minimum ($[CH_3-SiH_3-CH_3]^{\bullet}$). However, despite considerable effort, all attempts of optimizing the hypervalent minimum resulted in expulsion of one of the Si hydrogen atoms, leading to the formation of dimethylsilane. In the range 110−90°, the reaction proceeded directly to hydrogen expulsion from silicon, with activation energies ranging from 17.4 to 18.8 kcal mol^{-1}. The minimum barrier for the hydrogen expulsion reaction occurs at C−Si−C = 100° (Table 1), in agreement with the TS (**TS3**) optimized for reaction (3) above.

Similar to what was noted for the energy profile of the **D0** set of scans, the frontside S_H2 mechanism for reaction 1 is activated in the range 85° ≥ C−Si−C ≥ 60°. Again, the corresponding activation energies, 22.5−42.3 kcal mol^{-1}, are considerably higher than those found for the backside S_H2 reaction.

In summary, the constrained optimization scans performed in the present work indicate that reactions 1−3 may proceed in wide ranges of the C−Si−C angle. Both of the **D0** and **D180** sets of scans suggest that the backside S_H2 mechanism for reaction 1 is active within the approximate range 140−180°, with preference for the most linear C−Si−C angles. The scans indicate further that the energetically most feasible reaction, the hydrogen abstraction (2), proceeds in the range 90−135°, but only if methylsilane and the methyl radical are oriented such that the methyl radical approaches one of the hydrogen atoms at silicon. If, on the other hand, the methyl radical approaches the silicon atom in between two Si hydrogen atoms, the hydrogen abstraction reaction (2) does not occur at all. Instead, channels for hydrogen expulsion from silicon and, possibly, formation of a hypervalent minimum, become activated. Finally,

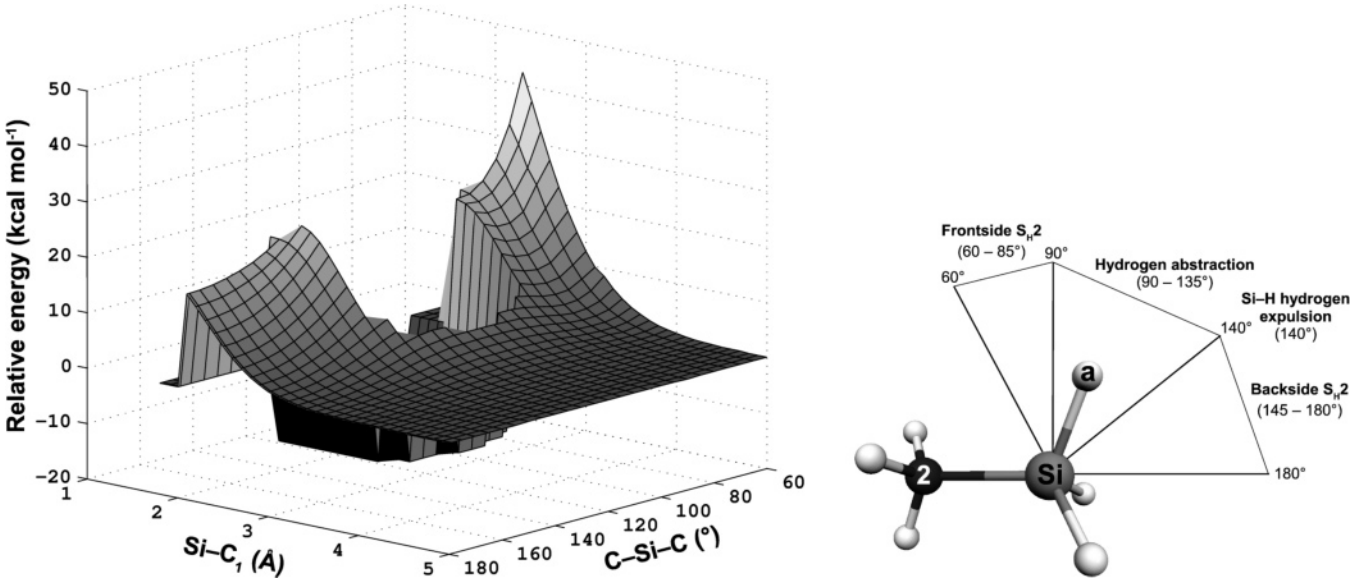

Figure 4. 2-dimensional plot of the energy *versus* the Si−C_1 distance and the C−Si−C angle for the B3LYP/6-31+G(d,p) constrained optimization scans in the **D0** set.

TABLE 1: Various Reactions Observed in the D0 and D180 Sets of Scans, Including Their Barriers, as Well as the C−Si−C Angles and Si−C_1 Distances Where They Proceed

	D0 set of scans			D180 set of scans		
C−Si−C (deg)	reaction	barrier (kcal mol^{-1})	Si−C_1 (Å)	reaction	barrier (kcal mol^{-1})	Si−C_1 (Å)
60	frontside S_H2	42.3	2.3	frontside S_H2	42.3	2.2
65	frontside S_H2	33.6	2.3	frontside S_H2	32.2	2.2
70	frontside S_H2	28.0	2.3	frontside S_H2	28.5	2.1
75	frontside S_H2	24.7	2.3	frontside S_H2	23.7	2.1
80	frontside S_H2	23.4	2.2	frontside S_H2	22.9	2.0
85	frontside S_H2	22.7	2.3	frontside S_H2	22.5	1.9
90	H abstraction	8.4	3.1	Si−H hydrogen expulsion	18.8	2.0
95	H abstraction	7.1	3.2	Si−H hydrogen expulsion	17.6	2.0
100	H abstraction	7.1	3.2	Si−H hydrogen expulsion	17.4	2.1
105	H abstraction	6.0	3.3	Si−H hydrogen expulsion	17.9	2.1
110	H abstraction	6.0	3.3	Si−H hydrogen expulsion	18.7	2.1
115	H abstraction	6.0	3.3	hypervalent minimum?	19.5	2.2
120	H abstraction	7.1	3.2	hypervalent minimum?	20.1	2.2
125	H abstraction	7.2	3.2	hypervalent minimum?	20.4	2.2
130	H abstraction	6.9	3.2	hypervalent minimum?	20.7	2.2
135	H abstraction	9.8	3.0	hypervalent minimum?	20.9	2.1
140	Si−H hydrogen expulsion	24.6	2.2	backside S_H2	21.6	2.0
145	backside S_H2	22.6	2.0	backside S_H2	21.6	2.1
150	backside S_H2	20.9	2.1	backside S_H2	21.6	2.1
155	backside S_H2	19.6	2.1	backside S_H2	21.4	2.1
160	backside S_H2	18.7	2.1	backside S_H2	21.0	2.1
165	backside S_H2	18.0	2.1	backside S_H2	18.8	2.2
170	backside S_H2	17.5	2.1	backside S_H2	18.4	2.2
175	backside S_H2	17.2	2.1	backside S_H2	18.1	2.2
179	backside S_H2	17.1	2.1	backside S_H2	18.0	2.2
179.9	backside S_H2	17.1	2.1	backside S_H2	18.0	2.2

at C−Si−C angles steeper than 90°, the frontside S_H2 mechanism for reaction 1 is activated. However, the corresponding barrier increases rapidly with decreasing angles of attack so that this mechanism seems to be of minor importance for the present S_H2 reaction.

Complexes Formed between SiH_3CH_3 and CH_3I. As shown above, the relative orientation of the methyl radical and the methylsilane molecule is crucial for the outcome of the reaction. A natural question to ask is therefore whether certain relative orientations of the methyl radical precursor (CH_3I) and the methylsilane molecule are more likely than others, due to the intermolecular interactions in the frozen matrix before irradiation.

A preliminary search for such weakly bound SiH_3CH_3/CH_3I complexes was performed with B97-1/6-31+G(d,p)/LanL2DZ. For this purpose, 38 constrained optimization scans were carried out to probe the PES for candidate complex structures when methyl iodide approached either the carbon or the silicon atom in methylsilane from different C−C−Si or C−Si−C angles (60°, 110°, and 180°). A total of 27 of these scans contained minima in their respective energy profile and the structure with the lowest energy in the respective scan was subsequently fully optimized with B97-1/6-311+G(2df,2p)/LanL2DZ. Out of the resulting 27 optimized structures, 11 unique complexes (**1**−**11**) could be identified. Moreover, when these 11 complexes were re-optimized at the MP2/6-311+G(2df,2p)/LanL2DZ level, complex **11** collapsed to complex **5**, and substantial changes in the geometry occurred for complex **2**. The 10 (11) optimized MP2 (B97-1) complexes are displayed in Figure 6 with selected geometrical parameters.

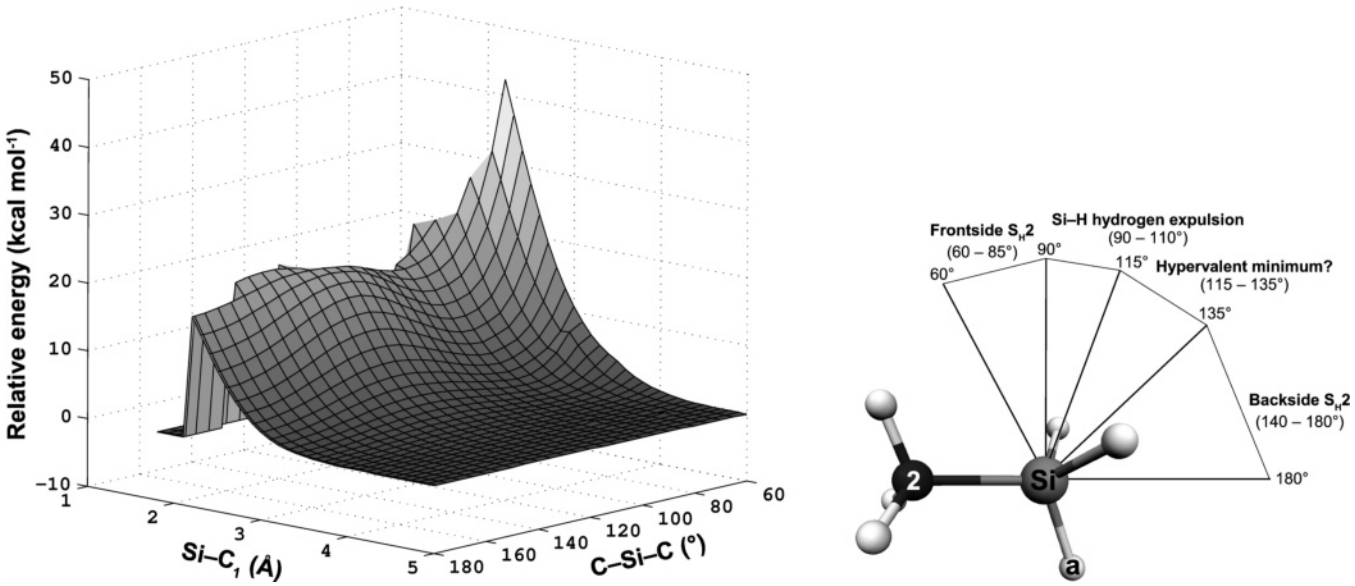

Figure 5. 2-dimensional plot of the energy *versus* the Si−C_1 distance and the C−Si−C angle for the B3LYP/6-31+G(d,p) constrained optimization scans in the **D180** set.

TABLE 2: Relative Energies, in kcal mol^{-1}, of the Complexes Located between Methyl Iodide and Methylsilane

	geometry optimization		single point at the MP2/6-311+G(2df,2p)/LanL2DZ optimized geometries	
	B97-1/ 6-311+G(2df,2p)/ LanL2DZ	MP2/ 6-311+G(2df,2p)/ LanL2DZ	CCSD(T)/ 6-311+G(2df,2p)/ LanL2DZ	CCSD(T)/ 6-311++G(3df,3pd)/ LanL2DZdp
1	0.00	0.00	0.00	0.00
2	0.78	0.38	0.45	0.77
3	0.58	0.63	0.65	0.95
4	0.46	1.40	1.51	1.25
5	0.64	0.95	0.99	1.27
6	0.79	1.05	1.11	1.27
7	0.58	1.47	1.60	1.47
8	0.92	1.16	1.16	1.71
9	0.70	1.72	1.83	1.72
10	0.96	2.00	2.11	2.15
11	0.79	*a*		

[a] This complex collapsed to **5** at the MP2 level.

In general, MP2 and B97-1 give similar qualitative predictions of the geometries of the present complexes. However, the intermolecular bond distances in complexes **1**, **3**, **5**, **6**, and **8** are overestimated by ca. 0.05−0.2 Å with B97-1 as compared with MP2. On the contrary, the intermolecular bond distances in **4**, **7**, **9**, and **10** are longer with MP2 compared with B97-1. As mentioned, the most noteworthy deviation in geometry between the two methods is found for complex **2**. At the B97-1 level, this complex has a conformation in which the methyl moiety in methyl iodide points toward the Si−C bond in methylsilane, whereas at the MP2 level, the two molecular fragments attain a nearly parallel conformation relative to one another with respect to the C−I and Si−C bonds (see Figure 6).

The electronic energies of the MP2 complexes were obtained with CCSD(T)/6-311+G(2df,2p)/LanL2DZ and CCSD(T)/6-311++G(3df,3pd)/LanL2DZdp. The former method measures the importance of adding additional electron correlation to the MP2 wavefunction, and the latter gives an indication of the basis set effect on the relative energies. The relative energies of the complexes at all levels of theory employed here are given in Table 2. Inspection of this table reveals some interesting facts. First, all methods predict that complex **1** is most and complex **10** least stable. Second, the difference in energy between complexes **10** and **1** is small at all levels of theory and B97-1 predicts the smallest energy difference, 0.96 kcal mol^{-1}, whereas MP2 and CCSD(T) give similar predictions of this energy difference, 2.00−2.15 kcal mol^{-1}. Interestingly, a comparison of the MP2 and CCSD(T) energies calculated with the 6-311+G-(2df,2p)/LanL2DZ basis set for all complexes reveals that the two methods are both qualitatively and quantitatively similar. MP2 and CCSD(T) with this basis set give the same relative ordering of the complexes and the maximum deviation in relative energy is only 0.13 kcal mol^{-1} (complex **7**). These facts suggest that the electron correlation provided by MP2 is sufficient for predicting accurate energies for the present complex type. In contrast, a similar comparison between the CCSD(T) energies computed with the larger 6-311++G(3df,-3pd)/LanL2DZdp basis set with those calculated with 6-311+G-(2df,2p)/LanL2DZ reveals larger deviations. For these levels, the maximum relative energy difference is 0.55 kcal mol^{-1} (complex **8**). Moreover, the relative ordering of the complexes are different. For instance, **4**, which is the fourth most stable complex with the largest basis set, is the seventh most stable with the smallest one, and complex **8**, which is the sixth most stable species with the smallest basis set, is the eighth most

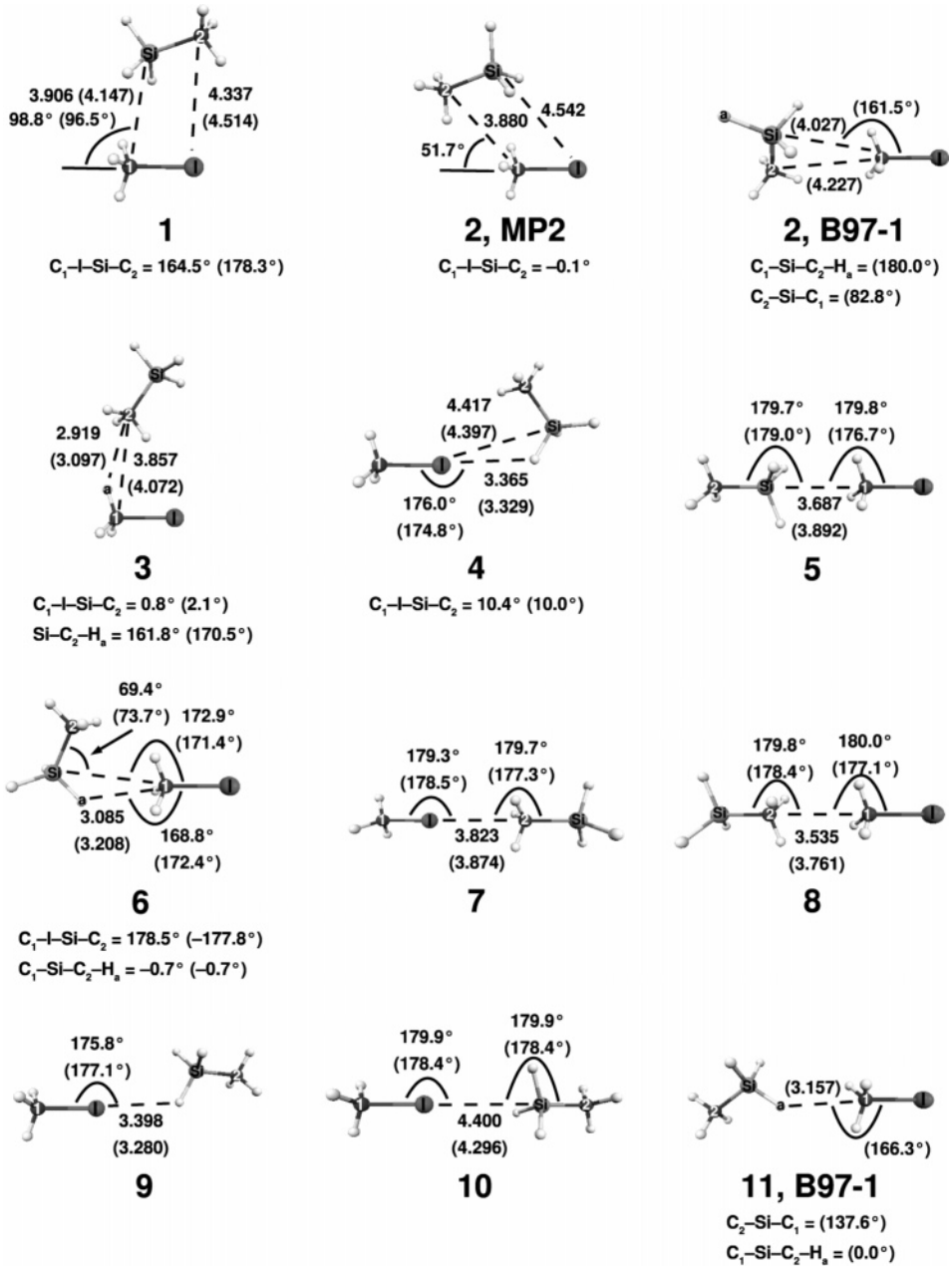

Figure 6. MP2 and B97-1 optimized complexes between methyl iodide and methylsilane. The 6-311+G(2df,2p)/LanL2DZ basis set was used in all computations. Bond lengths are given in Ångströms, and the B97-1 values are given within parentheses.

stable complex with the largest one. Thus, although the electron correlation effect is essentially converged with MP2, the use of a very large basis set seems to be important for the prediction of accurate energies for these type of complexes. The remaining discussion refers to the geometries optimized with MP2 and the energies calculated with CCSD(T)/6-311++G(3df,3pd)/LanL2DZdp, unless otherwise is noted.

By inspection of both Figure 6 and Table 2, one can see that the two MP2 complexes with the lowest energies, **1** (0.00 kcal mol^{-1}) and **2** (0.77 kcal mol^{-1}), have parallel arrangements with respect to the C−I and Si−C bonds and that the heavy atoms are essentially located in the same plane ($C_1-I-Si-C_2$ = +164.5° and −0.1°, respectively). Hence, the two species differ mainly in that the methylsilane is rotated ca. 180° in complex **2** relative to methyl iodide in **1**. In complex **3** (0.95 kcal mol^{-1}), methylsilane is again located above the C−I axis in methyl iodide, but for this complex the methyl moiety in methylsilane is directed toward a hydrogen (H_a in Figure 6) in methyl iodide.

Complexes **4**, **5**, and **6** are predicted to have almost the same energies (1.25, 1.27, and 1.27 kcal mol^{-1}, respectively). In **4**, the iodine atom in methyl iodide interacts with an Si hydrogen in methylsilane. In complex **5**, the molecular fragments attain the favorable collinear conformation for the backside S_H2 reaction (1), and in **6**, the methyl moiety in methyl iodide points approximately toward an Si hydrogen (H_a in Figure 6) in methylsilane, which is a favorable conformation for the hydrogen abstraction reaction (2).

Proceeding to the complexes with the highest energies, **7** (1.47 kcal mol^{-1}) and **8** (1.71 kcal mol^{-1}) are both collinear conformers where, in the former compound, the iodine points toward the carbon in methylsilane, but in the latter, the methyl moiety in methyl iodide is directed toward the same carbon. In complex **9** (1.72 kcal mol^{-1}), the C−I and Si−C bonds are close to parallel but this complex is stabilized by an interaction between the iodine atom and one Si hydrogen. Finally, in complex **10**, which has the highest energy (2.15 kcal mol^{-1}),

the conformation is again collinear, but now the iodine atom is directed toward the Si atom.

Of the different located complexes, **5** and **6** are of direct importance for the reactions observed in ESR spectroscopy,[7] *i.e.*, the S_H2 reaction (1) and the hydrogen abstraction (2). In particular, because **5** is almost perfectly collinear, photodissociation of methyl iodide in this complex would lead to methyl radical attack at silicon with an approximate C−Si−C angle of 180°. Bearing in mind that this angle was found to be the most favorable attack angle for the backside S_H2 reaction (1), it seems likely that this complex could account for a large fraction of the observed[7] S_H2 reactions. As for complex **6**, whereas this compound indeed has the most favorable conformation for the hydrogen abstraction reaction (2) of all complexes optimized with MP2, a detailed inspection of Figure 6 reveals, nevertheless, that it is not perfect in this sense. This is reflected by the fact that $H_a-C_1-I = 168.8°$, which implies that the methyl moiety in methyl iodide is not directed exactly toward an Si hydrogen, but rather points toward the $Si-H_a$ bond. Moreover, the C−Si−C angle in this complex, 69.4°, is very steep. Because it was found above that the hydrogen abstraction reaction (2) proceeded favorably only in the range $90° \leq C-Si-C \leq 135°$ (Table 1), this could indicate that photodissociation of methyl iodide in **6** might not lead to hydrogen abstraction with full efficiency. Finally, it is interesting to note that the B97-1 complex **11**, which also has a molecular arrangement in favor of the hydrogen abstraction from silicon, becomes unstable at the MP2 level. Indeed, with MP2, complex **11** collapsed to **5**. Because MP2, in general, is preferable over DFT for weakly interacting systems, and because the B97-1 optimized C−Si−C angle in **11** is rather steep, 137.6°, the stability of the molecular arrangement in **5** with respect to deviations in this angle from linearity seems to be significant.

Conclusions

By means of ESR spectroscopy, we recently observed that the S_H2 type reaction of deuterated methyl radicals ($^{\bullet}CD_3$) with deuterated methylsilane (SiD_3CH_3) (eq B) proceeded with high selectivity over the competitive deuterium abstraction reaction from the SiD_3 moiety immediately after photolysis of CD_3I.[7] The large kinetic isotope effect for the hydrogen abstraction from methylsilane ($k_{Si-H}/k_{Si-D} = 5200$ at 77 K),[9] leading to slow deuterium abstraction, was proposed to explain the experimental results. However, complementary quantum chemical calculations indicated that the barriers for the S_H2 reaction and hydrogen abstraction, which were found to be 22.7 and 8.8 kcal mol^{-1} (25.7 and 10.8 kcal mol^{-1} in the present work) starting from the unlabeled reactants in (B), were very similar for the deuterated reactants, 22.0 and 8.8 kcal mol^{-1}, respectively.[7] This suggested that the hydrogen abstraction would be the favored reaction, regardless of the isotopic identity of the hydrogens in the system. Nevertheless, an estimation of the translational kinetic energy of the methyl radical following photolysis of methyl iodide (∼22 kcal mol^{-1}) indicated that the S_H2 reaction might proceed given a favorable initial orientation of methylsilane and methyl iodide.[7]

In the present work, we continue to investigate the cause of the observed S_H2 reaction between the methyl radical and methylsilane by means of quantum chemical calculations. In particular, an extensive search for different SiH_3CH_3/CH_3I complexes was here undertaken, and we investigate the angular flexibility with respect to deviations in the C−Si−C angle for the different reactions between $^{\bullet}CH_3$ and SiH_3CH_3 when the methyl radical approaches the silicon atom.

From the latter calculations, it is found that the backside mechanism for the S_H2 reaction may proceed favorably in a wide range of C−Si−C angles, 140−180°, whereas the hydrogen abstraction reaction is active in the range 90−135°. For steeper C−Si−C angles, the frontside S_H2 mechanism is activated. However, the latter mechanism is probably unimportant for the present S_H2 reaction due to high barriers along its reaction paths.

The search for SiH_3CH_3/CH_3I complexes resulted in 10 different conformers at the MP2/6-311+G(2df,2p)/LanL2DZ level. Interestingly, one of these complexes, **5**, was found to correspond to the collinear arrangement where the methyl moiety in methyl iodide points toward the silicon atom in methylsilane, which is the most favorable conformation for the subsequent S_H2 reaction with the backside mechanism. It was also found that this complex seems to be rather stable toward deviations from linearity with respect to the C−Si−C angle. Moreover, at the CCSD(T)/6-311++G(3df,3pd)/LanL2DZdp level, the molecular arrangement in **5** was predicted to be the lowest energy collinear conformer. One complex, **6**, was located to be a favorable orientation for the hydrogen abstraction. However, in this complex, the C−Si−C angle is very steep, 69.4°. Because it was found that the hydrogen abstraction reaction proceeded favorably only in the range $90° \leq C-Si-C \leq 135°$, photodissociation of methyl iodide in **6** might not lead to hydrogen abstraction with full efficiency.

Thus, the data here calculated for the reactions between the methyl radical and methylsilane, coupled with the structural and energetic properties of SiH_3CH_3/CH_3I complexes formed prior to photolysis of methyl iodide, might provide a reasonable explanation of the observed S_H2 reaction between the methyl radical and methylsilane.

Acknowledgment. This work was supported by the Wenner-Gren Foundation. We thank the Swedish National Supercomputer Center (NSC) for generous allocation of computer time.

Supporting Information Available: Absolute B3LYP SCF and ZPVE as well as CCSD(T) energies of the B3LYP optimized stationary points involved in the reactions between the methyl radical and methylsilane. Absolute energies at the various levels of theory of the MP2 and B97-1 optimized SiH_3CH_3/CH_3I complexes; *xyz*-matrices of all located stationary points. This material is available free of charge via the Internet at http://pubs.acs.org.

References and Notes

(1) Ingold, K. U.; Roberts, B. P. *Free-Radical Substitution Reactions*; Wiley-Interscience: New York, 1973.

(2) Davies, A. G.; Roberts, B. P. Bimolecular homolytic substitution at metal centers. In *Free Radicals*; Kochi, J. K., Ed.; Wiley-Interscience: New York, 1973; Vol. 1, pp 547−587.

(3) Fossey, J.; Lefort, D.; Sorba, J. *Free Radicals in Organic Chemistry*; John Wiley & Sons: Chichester, U.K., 1995; pp 123−137.

(4) Walton, J. C. *Acc. Chem. Res.* **1998**, *31*, 99−107.

(5) Schiesser, C. H; Wild, L. M. *Tetrahedron* **1996**, *52*, 13265−13314.

(6) Turecek, F. Transient intermediates of chemical reactions by neutralization-reionization mass spectroscopy. In *Modern Mass Spectroscopy*; *Topics in Current Chemistry*, Vol. 225; Schalley, C. A., Ed.; Springer: Berlin, 2003.

(7) Komaguchi, K.; Norberg, D.; Nakazawa, N.; Shiotani, M.; Persson, P.; Lunell, S. *Chem. Phys. Lett.* **2005**, *410*, 1−5.

(8) Wisniowski, P.; Bobrowski, K.; Carmichael, I.; Hug, G. L. *J. Am. Chem. Soc.* **2004**, *126*, 14468−14474.

(9) Komaguchi, K.; Ishiguri, Y.; Tachikawa, H.; Shiotani, M. *Phys. Chem. Chem. Phys.* **2002**, *4*, 5276−5280.

(10) Schiesser, C. H.; Styles, M. L.; Wild, L. M. *J. Chem. Soc., Perkin Trans. 2* **1996**, 2257−2262.

(11) Horvat, S. M.; Schiesser, C. H.; Wild, L. M. *Organometallics* **2000**, *19*, 1239−1246.
(12) Matsubara, H.; Horvat, S. M.; Schiesser, C. H. *Org. Biomol. Chem.* **2003**, *1*, 1199−1203.
(13) Frisch, M. J.; Trucks, G. W.; Schlegel, H. B.; Scuseria, G. E.; Robb, M. A.; Cheeseman, J. R.; Montgomery, J. A., Jr.; Vreven, T.; Kudin, K. N.; Burant, J. C.; Millam, J. M.; Iyengar, S. S.; Tomasi, J.; Barone, V.; Mennucci, B.; Cossi, M.; Scalmani, G.; Rega, N.; Petersson, G. A.; Nakatsuji, H.; Hada, M.; Ehara, M.; Toyota, K.; Fukuda, R.; Hasegawa, J.; Ishida, M.; Nakajima, T.; Honda, Y.; Kitao, O.; Nakai, H.; Klene, M.; Li, X.; Knox, J. E.; Hratchian, H. P.; Cross, J. B.; Bakken, V.; Adamo, C.; Jaramillo, J.; Gomperts, R.; Stratmann, R. E.; Yazyev, O.; Austin, A. J.; Cammi, R.; Pomelli, C.; Ochterski, J. W.; Ayala, P. Y.; Morokuma, K.; Voth, G. A.; Salvador, P.; Dannenberg, J. J.; Zakrzewski, V. G.; Dapprich, S.; Daniels, A. D.; Strain, M. C.; Farkas, O.; Malick, D. K.; Rabuck, A. D.; Raghavachari, K.; Foresman, J. B.; Ortiz, J. V.; Cui, Q.; Baboul, A. G.; Clifford, S.; Cioslowski, J.; Stefanov, B. B.; Liu, G.; Liashenko, A.; Piskorz, P.; Komaromi, I.; Martin, R. L.; Fox, D. J.; Keith, T.; Al-Laham, M. A.; Peng, C. Y.; Nanayakkara, A.; Challacombe, M.; Gill, P. M. W.; Johnson, B.; Chen, W.; Wong, M. W.; Gonzalez, C.; Pople, J. A. *Gaussian 03*, revision C.02; Gaussian, Inc.: Wallingford, CT, 2004.
(14) Flükiger, P.; Lüthi, H. P.; Portmann, S.; Weber, J. MOLEKEL-4.3, Swiss Center for Scientific Computing, Manno, Switzerland, 2000.
(15) Kristyán, S.; Pulay, P. *Chem. Phys. Lett.* **1994**, *229*, 175−180.
(16) Ruiz, E.; Salahub, D. R.; Vela, A. *J. Am. Chem. Soc.* **1995**, *117*, 1141−1142.
(17) Hobza, P.; Sponer, J.; Reschel, T. *J. Comput. Chem.* **1995**, *16*, 1315−1325.
(18) Shiotani, M.; Isamoto, N.; Hayashi, M.; Fängström, T.; Lunell, S. *J. Am. Chem. Soc.* **2000**, *122*, 12281−12288.
(19) Zhao, Y.; Truhlar, D. G. *J. Chem. Theory. Comput.* **2005**, *1*, 415−432.
(20) Check, C. E.; Faust, T. O.; Bailey, J. M.; Wright, B. J.; Gilbert, T. M.; Sunderlin, L. S. *J. Phys. Chem. A* **2001**, *105*, 8111−8116.
(21) This criterion is obtained by the Int(Grid=UltraFine) option in Gaussian03.